Neurobiology of Aging 34 (2013) 1825–1836

Contents lists available at SciVerse ScienceDirect

Neurobiology of Aging

journal homepage: www.elsevier.com/locate/neuaging

Regional differences in gene expression and promoter usage in aged human brains

Luba M. Pardo [a,1], Patrizia Rizzu [a,1], Margherita Francescatto [a,b], Morana Vitezic [c,d], Gwenaël G.R. Leday [e], Javier Simon Sanchez [a], Abdullah Khamis [f], Hazuki Takahashi [c], Wilma D.J. van de Berg [g], Yulia A. Medvedeva [f], Mark A. van de Wiel [h], Carsten O. Daub [c], Piero Carninci [c], Peter Heutink [a,c,*]

[a] Section Medical Genomics, Department of Clinical Genetics, VU University Medical Center, Amsterdam, The Netherlands
[b] GABBA Program, Instituto de Ciências Biomédicas Abel Salazar, UP, Porto, Portugal
[c] RIKEN Omics Science Center, RIKEN Yokohama Institute, Yokohama, Japan
[d] Department of Cell and Molecular Biology (CMB), Karolinska Institute, Stockholm, Sweden
[e] Department of Mathematics, VU University, Amsterdam, The Netherlands
[f] Computational Bioscience Research Center, King Abdullah University of Science and Technology, Thuwal, Saudi Arabia
[g] Department of Anatomy and Neurosciences, Section Functional Neuroanatomy, Neuroscience Campus Amsterdam, VU University Medical Center, Amsterdam, The Netherlands
[h] Department of Epidemiology and Biostatistics, VU University Medical Center, Amsterdam, The Netherlands

ARTICLE INFO

Article history:
Received 27 August 2012
Received in revised form 29 November 2012
Accepted 7 January 2013
Available online 19 February 2013

Keywords:
CAGE
Brain transcriptome
Aging

ABSTRACT

To characterize the promoterome of caudate and putamen regions (striatum), frontal and temporal cortices, and hippocampi from aged human brains, we used high-throughput cap analysis of gene expression to profile the transcription start sites and to quantify the differences in gene expression across the 5 brain regions. We also analyzed the extent to which methylation influenced the observed expression profiles. We sequenced more than 71 million cap analysis of gene expression tags corresponding to 70,202 promoter regions and 16,888 genes. More than 7000 transcripts were differentially expressed, mainly because of differential alternative promoter usage. Unexpectedly, 7% of differentially expressed genes were neurodevelopmental transcription factors. Functional pathway analysis on the differentially expressed genes revealed an overrepresentation of several signaling pathways (e.g., fibroblast growth factor and *wnt* signaling) in hippocampus and striatum. We also found that although 73% of methylation signals mapped within genes, the influence of methylation on the expression profile was small. Our study underscores alternative promoter usage as an important mechanism for determining the regional differences in gene expression at old age.

1. Introduction

The brain is the most complex organ of the human body, and this complexity is a major landmark of human evolution (Konopka and Geschwind, 2010). The brain can be divided into different functional and anatomic regions that are established during development and maintained throughout life. The mechanisms that regulate normal brain function and differentiation are controlled by both genetic (Johnson et al., 2009) and epigenetic factors (Miller and Sweatt, 2007), and alterations in these mechanisms can lead to neurodegenerative diseases (Abdolmaleky et al., 2005). There have been tremendous advances in our understanding of the molecular mechanisms involved in brain function, and the regional differences in these functions are beginning to be understood (Khaitovich et al., 2004; Roth et al., 2006). Less is known about the genetic mechanisms that are responsible for establishing and maintaining these differences throughout development, adulthood, and aging. Insights into these mechanisms are required to understand the differential susceptibility of distinct brain regions to neuronal insults (Double et al., 2010). For example, the genes for which mutations have been characterized in Alzheimer's disease (AD) (Joachim et al., 1989; Shen et al., 1997) and Parkinson's disease (PD) (Bandopadhyay et al., 2004) are often ubiquitously expressed whereas the observed pathology is restricted to specific brain regions and specific cell types (Double et al., 2010). Dissection of the molecular basis of this selective vulnerability will be pivotal to our understanding of disease pathogenesis and the development of specific therapies.

Much of our current insight into the molecular basis of brain function results from detailed studies of single genes or

* Corresponding author at: Department of Clinical Genetics, VU University Medical Center, van der Boechorststraat, 71081 BT Amsterdam, The Netherlands. Tel.: +31-205989962; fax: +31-2059983596.
E-mail address: p.heutink@vumc.nl (P. Heutink).
[1] These authors contributed equally to this work.

0197-4580
http://dx.doi.org/10.1016/j.neurobiolaging.2013.01.005

molecular mechanisms often initiated by the identification of genetic mutations (Hardy and Selkoe, 2002). However, unbiased approaches, where large numbers of genes are assessed simultaneously, are expected to be more powerful to dissect the genetic mechanisms controlling brain function. Large-scale analysis of gene expression in brain was pioneered by microarray experiments (Khaitovich et al., 2004). In recent years, high-throughput sequence-based technologies have been developed to analyze the mammalian transcriptome in more detail and at greater depth (Sandelin et al., 2007). These technologies have been decisive to uncover a complex picture of the mammalian transcriptome (Carninci et al., 2005) and to identify new mechanisms of gene regulation and control of gene expression in brain (Kang et al., 2011; Tollervey et al., 2011). Among sequence-based technologies, tag-based approaches such as cap analysis of gene expression (CAGE) have been used to comprehensively profile the transcription start sites (TSSs) and the promoter regions (Takahashi et al., 2012). CAGE is a cap-trapping–based method that profiles 5′ capped transcripts of both coding and noncoding RNA classes and has been pivotal in the discovery of alternatively regulated TSSs and novel regulatory elements (Carninci et al., 2006; Valen et al., 2009).

To understand how different promoters and control elements of genes establish and maintain region-specific expression patterns, we used CAGE in combination with massive parallel sequencing to profile TSSs of brain regions in 7 aged healthy individuals, at a genome-wide scale. We selected 5 samples of caudate nuclei, putamen, frontal and temporal cortices, and hippocampus, which are specifically vulnerable in the most prevalent neurodegenerative disorders (Double et al., 1996). First, we characterized the transcriptome of aged human brain and evaluated the extent of alternative promoter usage. Second, we quantified differences in gene expression and promoter usage across 5 brain regions. Finally, we analyzed the extent to which methylation influenced the observed expression profiles.

2. Methods

2.1. Brain specimens

The postmortem brain tissues were obtained from the Netherlands Brain Bank (Amsterdam, The Netherlands). The donors were aged subjects (age range: 70–91 years) without clinical signs of neurodegenerative or psychiatric disorders. All brains were neuropathologically evaluated by an experienced neuropathologist and classified for neurofibrillary tangles stage 0–VI (Alafuzoff et al., 2008), amyloid-beta plaques score 0–C, and Braak α-synuclein stage 0–VI using the staging protocols of Brain Net Europe and Braak (Alafuzoff et al., 2009a, 2009b; Braak et al., 2006). The dissection of the caudate, putamen, hippocampus, middle frontal gyrus (F2), and middle temporal gyrus regions was performed from snap frozen human brain sections. Tissue was stored at −80 °C until further processing. Pathologic examination of the brain specimens showed changes consistent with the age of the individuals. The age at death, cause of death, and postmortem delay until dissection are provided in Supplementary Table 1.

2.2. CAGE library preparation

Total RNA was extracted and purified from tissues using the Trizol tissue kit according to the instructions provided by the manufacturer (Invitrogen). RNA quality per library was assessed using the RNA integrity number with the Agilent Total RNA Nano kit (Table 1). The standard CAGE protocol (Kodzius et al., 2006) was adapted for sequencing on an Illumina platform. A thorough description of the protocol to prepare CAGE libraries and to sequence CAGE tags is presented in Takahashi et al. (2012). Briefly, complementary DNA (cDNA) was synthesized from total RNA using random primers, and this process was carried out at high temperature in the presence of trehalose and sorbitol to extend

Table 1
Description of the tag counts per region/sample

Individual	Region	Batch[a]	RIN	Tag counts[b]	Unique counts[c]	Mapping rate[d]	Ribosome mapping[e]
1	**Caudate**	**1**	7.6	1,988,794	935,084	0.856	0.062
1	**Frontal**	**1**	7	3,453,682	1,531,751	0.866	0.049
1	**Hippocampus**	**1**	6.5	2,022,640	979,162	0.811	0.09
1	**Putamen**	**1**	7.7	3,814,753	1,627,659	0.826	0.069
1	**Temporal**	**1**	6.3	4,333,255	1,937,270	0.822	0.07
2	**Hippocampus**	**1**	6.5	1,682,943	310,481	0.843	0.072
2	**Caudate**	**2**	7.2	1,663,688	362,468	0.724	0.088
2	**Frontal**	**2**	6.9	1,745,155	801,757	0.822	0.04
2	**Putamen**	**2**	6.5	1,216,441	274,776	0.702	0.113
2	**Temporal**	**2**	6.8	936,396	259,968	0.748	0.103
3	**Frontal**	**2**	7.1	2,111,277	505,207	0.779	0.068
3	**Hippocampus**	**2**	8.8	1,785,386	413,336	0.816	0.041
3	**Temporal**	**2**	6.8	1,103,935	255,621	0.84	0.041
4	**Temporal**	**2**	5.9	1,199,974	356,840	0.71	0.127
4	**Frontal**	**2**	6.5	2,035,347	472,327	0.739	0.107
4	**Hippocampus**	**2**	6.4	1,251,589	335,644	0.731	0.109
4	**Putamen**	**2**	6.5	2,541,166	516,842	0.73	0.121
5	**Caudate**	**1**	7.9	3,096,524	1,144,105	0.875	0.059
5	**Putamen**	**1**	6.6	4,029,122	1,541,543	0.834	0.082
6	**Caudate**	**1**	7.4	3,587,220	1,296,765	0.875	0.053
6	**Putamen**	**1**	6.3	2,085,385	795,569	0.868	0.072
7	**Caudate**	**1**	6.8	4,875,578	1,625,317	0.862	0.062
7	**Frontal**	**2**	6.2	2,324,932	407,993	0.731	0.111
7	**Hippocampus**	**2**	6.2	3,158,604	597,669	0.775	0.033
7	**Temporal**	**2**	6.2	1,104,711	241,508	0.699	0.157

Details on the quality control and final counts used for the analysis are presented in Supplementary data. Individual, region and batch id are presented in bold.
Key: RIN, RNA integrity number.
[a] Refers to 2 main batch effects corresponding to different period of times in which the cap analysis of gene expression libraries were prepared (Supplementary data).
[b] Refers to the total tag counts after removal of sequencing artifacts.
[c] Refers to the tag counts that map to single positions in the genome unique regions.
[d] Refers to proportion of tags that mapped to less than 10 positions.
[e] Refers to the proportion of tags that mapped to ribosomal DNA.

cDNA synthesis through GC-rich regions in 5′ untranslated regions (UTRs). The 5′ ends of messenger RNA within RNA-DNA hybrids were selected by the cap-trapper method (Kodzius et al., 2006) and ligated to a linker so that an EcoP15I recognition site was placed adjacent to the start of the cDNA, corresponding to the 5′ end of the original messenger RNA. This linker was used to prime second-strand cDNA synthesis. Subsequent EcoP15I digestion released the 25- to 27-base pair (bp) CAGE tags. After ligation of a second linker, CAGE tags were polymerase chain reaction amplified, purified, and sequenced on the Illumina Genome Analyzer GLXII platform (Takahashi et al., 2012). The data have been submitted to the Gene Expression Omnibus (GEO) public repository (GSE43472).

2.3. DNA methylation microarrays

DNA isolation and purification to detect methylation was carried out following standard protocols (Supplementary data, Methods). Genome-wide amplified input and output samples were sent to Roche NimbleGen where they were hybridized to DNA Methylation 2.1 Million Deluxe Promoter Arrays. The arrays have a mean probe spacing of 99 bp and median probe spacing of 100 bp. Each array has more than 2.1million probes distributed in the following manner (1) promoter regions from 7250 bases upstream of each TSS to 3250 bases downstream; (2) micro RNA (miRNA) genes, starting from 15 kbp upstream of the mature gene product to its 3′ end; (3) CpG islands; and (4) ENCODE regions. Probes were chosen from the hg18 tiling database. Therefore, the probes targeted mainly annotated promoter regions and CpG islands.

2.4. Bioinformatics and statistical analysis of CAGE data

Primary quality control analysis included the removal of linker and barcode sequences as well as other sequencing artifacts to obtain raw CAGE tags of approximately 27 bps. Next, raw CAGE tags were mapped to the human genome (hg18 build) using Nexalign (T. Lassmann, http://genome.gsc.riken.jp/osc/english/dataresource/) allowing for 1 mismatch and 1 indel. The above steps were carried out with scripts and software (see Lassmann et al., 2009) developed at the RIKEN. Following previous approaches to analyze promoter activity based on CAGE data, we grouped raw CAGE tags into CAGE clusters using a clustering pipeline from Omics Science Center bioinformatics at the RIKEN (De Hoon et al., 2010). In brief, the CAGE tags that mapped to the same position in the human genome and were on the same strand were considered CAGE Transcription Start Sites (CTSSs) (level 1 [L1]). For tags that mapped to multiple positions in the genome, a rescuing approach was applied (Faulkner et al., 2008). L1 CAGE tags were clustered into level 2 tag clusters (L2 TCs) if they overlapped within 20 bps and were on the same strand. L2 TCs were grouped into level 3 (L3) TCs if they overlapped within a region of 400 bps and were on the same strand. For clarity, a CTSS marks the first nucleotide that is transcribed into RNA and is considered a putative TSS, whereas a L3 TC encompasses the region that is shared between proximal TSSs (Supplementary data, Methods) (Sandelin et al., 2007). After clustering approach, we obtained 6,735,699 CTSSs (L1 clusters). To increase the probability of capturing genuine promoter regions, we only selected L3 TCs that were present in at least 2 CAGE libraries and with a minimum count of 5 tags per million (TPM) (De Hoon et al., 2010) in at least 1 library; for example, only CTSS present at $\geq$5 TPM in one library and $\geq$1 TPM in another were included. For all downstream analysis, we used the L3 TCs. Unless stated otherwise, TCs refer to the L3 TCs.

Next, we annotated TCs to human genes by mapping the coordinates of the TCs to all available transcripts from GENCODE version 3d. To do this, we downloaded all GENCODE transcripts from the UCSC genome browser (hg18 build; University of California, Santa Cruz, CA [UCSC]) at different levels of validation (http://genome.ucsc.edu/cgi-bin/hgTables). Custom Perl scripts and BEDTools (Quinlan and Hall, 2010) were used to map the coordinates of the TCs to genomic regions corresponding to specific transcriptional units (Carninci et al., 2006). TCs that did not map to a specific gene were considered intergenic. Further, we divided the TCs into mutually exclusive classes according to the gene region they mapped to. TCs that mapped to a 5′ UTR or −300/+100 bps of a known TSS (core promoter region) were labeled as canonical. The remaining noncanonical TCs were labeled as 5′ UTR antisense, 3′ UTR, 3′ UTR antisense, intronic, exonic, intronic antisense, and exonic antisense.

We classified the genes to which the TCs mapped to according to the following Biotypes: protein-coding gene (if it had an open reading frame), long noncoding RNA (lncRNA), miRNA, pseudogene, processed transcript (no open reading frame, but transcribed and not classified into any other category), and other ncRNAs using the definitions from GENCODE (Harrow et al., 2006) (http://www.gencodegenes.org/gencode_biotypes.html).

2.4.1. Differential gene expression and promoter usage derived from CAGE data across 5 brain regions

To obtain an overview of the expression (count) profile of the CAGE libraries, we first tested for differential expression across brain regions and subsequently identified patterns of differences between these regions by means of hierarchical clustering. We focused on autosomal TCs with a minimum of 9 tag counts per TC because this is the minimum number of counts needed to get reliable estimate of expression (Robinson et al., 2010). We built a model that takes into account both biological and technical variations, as we found that tag expression was subject to batch effects (Supplementary data, Results). The model assumes that CAGE tag counts (y_{ij}) follow a negative binomial distribution, which is standard for modeling read/tag counts. It also includes brain group (5 levels corresponding to 5 regions), batch (2 levels corresponding to 2 main batches [Supplementary data, Results]), and individual (7 levels corresponding to 7 individuals) as covariates. Details of the mathematical and statistical procedure are presented in Supplementary data, Methods.

To identify differentially expressed TCs (DETC) showing similar differences among (a subset of) groups, we carried out hierarchical clustering (with Euclidean distance) based on the coefficients of brain regions, which are lower than 3 in absolute value. This was carried out with the R function hclust from package stats (with default agglomeration method). We chose the partition that maximized the average silhouette index width.

Functional enrichment analysis was subsequently done on clusters (modules) of DETCs using the PANTHER version 7.0 database (Supplementary data, Methods). All further functional pathway analyses were carried out using this database.

2.5. Bioinformatics and statistical analysis of methylation data

The log2 ratio of the probe intensity in the experimental sample against control DNA was determined. The log2 methylation signals were converted into methylation peaks (MPs) using the NimbleGen software (Roche) with default parameters (Supplementary data, Methods). Further, we removed MPs that mapped to X and Y chromosomes as well as those that overlapped with centromeres, telomeres, and segmental duplications. MPs overlapping with regions in which more than 1 segment was detected for a single sample were also removed. Next, we selected consensus MPs that were shared in a minimum of 2 samples. For this, we used the plink

software version 7 (Purcell et al., 2007) and identified shared methylated "segments" with the command: plink file –segment-group. Next, we used BEDTools (Quinlan and Hall, 2010) to map the MPs to annotated human genes (hg18) using GENCODE version 3d at different levels of annotation. We also mapped the MPs to CpG islands downloaded from UCSC browser (Fujita et al., 2011). Details of the experimental protocol and the downstream analysis are presented in Supplementary data.

2.5.1. Differential methylation analysis

We modeled the log2 ratios of the probe intensities taking both biological and technical variations into account and assuming that the ratios followed a normal distribution. Brain group (here we used the caudate as reference group), batch, and individual factors were covariates. We fitted 2 models per methylation probe: a full model, which included all 3 covariates and a null model where the factor brain group was discarded. We tested for differences in the models using a one-way analysis of variance, implemented in R version 13, and adjusted for multiple testing using the Bonferroni correction. Differentially methylated peaks (DMPs) were defined as differentially methylated probes occurring at a minimum overlap of 300 bps (R script provided by K. Lo at Roche, k.lo@roche.com).

2.5.2. Correlation between methylation signals and expression

First, we calculated the average methylation for every MP, adjusting for both biological and technical variations as mentioned previously. Next, we overlapped the genomic coordinates of the MPs with the genomic coordinates of the TCs (−1500/+500) using BEDTools (Quinlan and Hall, 2010) and estimated the Spearman correlation between the average mean intensity of methylation and the average expression of the overlapping TCs (geometric mean).

To test whether the expression of individual TCs were affected by methylation, we used the same statistical framework that we used to identify DETCs but included the methylation covariate as the variable of interest. Briefly, for each TC, we fitted 2 models. A full model with brain group, batch, and methylation as covariates, and a null model where methylation was removed. Because of the small number of MPs overlapping TCs, we could not fit the individual covariate. Significant differences were calculated as above.

3. Results

Supplementary Fig. 1 shows a schema of the main steps of experimental procedure and the data analysis we carried out in this study. We prepared 25 CAGE libraries from total RNA isolated from the caudate nuclei, putamen, frontal and temporal lobes, and hippocampus from the 7 donors. In total, we sequenced 72 million CAGE tags (1–2 million per library approximately) in 5 sequencing rounds. Table 1 summarizes the tag count and mapping rate per library after quality control (Supplementary data, methods). The final set of L3 TCs that were available for analysis numbered 70,202.

3.1. Features of brain transcriptome of aged individuals derived from CAGE

We mapped the TCs to 16,888 human genes from the GENCODE database (Raney et al., 2011). Fig. 1a shows that 31.2% of TCs mapped to the 5′ UTR or promoter regions of previously annotated transcripts (canonical TCs), whereas the remaining 68.9% mapped to other regions including introns, exons, and 3′ UTRs (noncanonical TCs). In addition, 13.6% of TCs did not map to any known transcript and were considered intergenic. Of these TCs, 559 (6%) mapped to lncRNAs (Jia et al., 2010) (Supplementary Table 2). Although canonical TCs represented less than one-third of all TCs (Fig. 1a), their expression was high and accounted for most of the overall TC

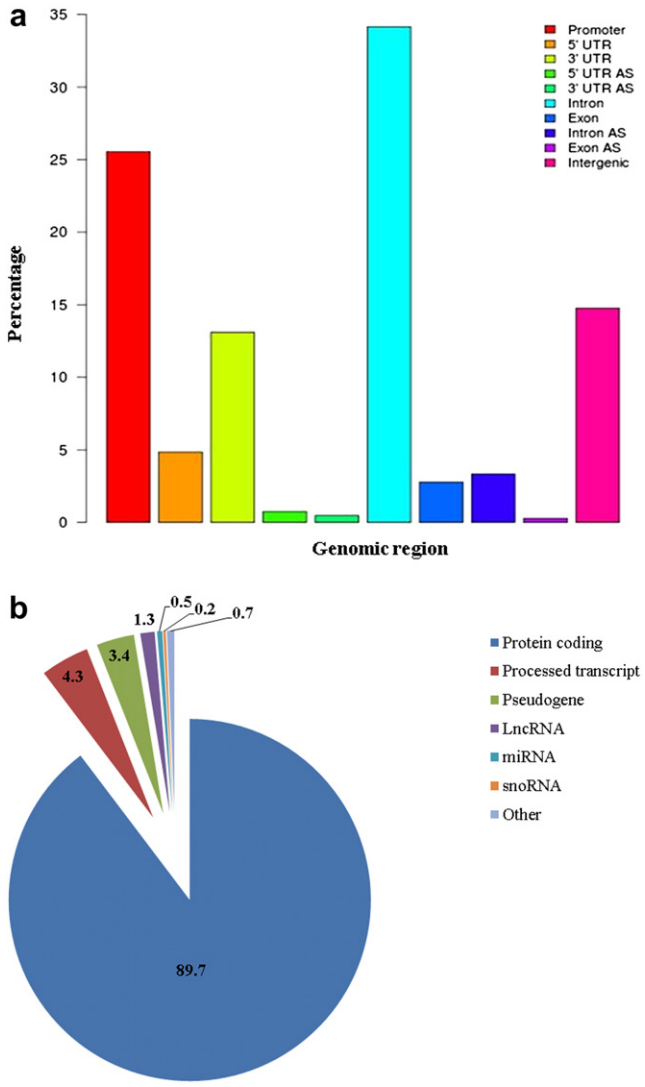

Fig. 1. Annotation of level 3 (L3) cap analysis of gene expression (CAGE) tag clusters (TCs) to human genes. (a) Barplot showing the percentage of TCs (y-axis) that map to different gene regions: promoters, 5′ untranslated regions (UTRs), 3′ UTRs, antisense, introns, exons, antisense introns, antisense exons, antisense 5′ UTR, antisense 3′ UTR, and outside genes (intergenic). Promoter regions were defined as −300/100 base pairs relative to the 5′ UTR. We defined canonical TCs those that mapped to promoters or 5′ UTRs. The TCs that mapped to other regions were classified as noncanonical. The proportion of canonical TCs represents one-third of all TCs we identified. (b) Distribution of biotype classes for genes with canonical L3 CAGE TCs. Pie chart showing the percentage of genes with at least 1 canonical TC classified by biotype class: protein-coding genes (gene with open reading frame), long noncoding RNAs (lncRNAS), pseudogenes, micro RNAs (miRNA), small nucleolar RNAs (snoRNA), and processed transcripts (no open reading frame but transcribed and not classified into any other category).

expression. In contrast, the expression of most noncanonical TCs was low (Supplementary Fig. 2).

Of all the expressed genes, 14,479 (87%) had canonical TCs (Supplementary data, Data set 1). As shown in Fig. 1b, 90% of these genes encode proteins. The remaining 10% consist of ncRNA, of which annotated pseudogenes account for 33%. We compared the list of genes that were expressed in our data set with those from RNASeq data from brain and other tissues (Ramskold et al., 2009). We found an overlap of 77% (Supplementary Fig. 3). Genes expressed in brain according to Ramskold et al. (2009) that were not present in our CAGE data set included both mitochondrial (e.g., *MT-ATP6*, *MT-ND3*, and *MT-CO2*) and ribosomal genes. In contrast,

there was a larger proportion of ncRNA in our brain CAGE data set (24% more compared with RNASeq, Supplementary Fig. 3b), with a particular enrichment for pseudogenes and lncRNAs.

We looked at the expression profile of 1909 highly expressed genes with canonical TCs (90th percentile of the log geometric mean of expression distribution; Supplementary Table 3) in more detail. This group included genes involved in brain aging (e.g., *GPAFP*, *SPARCL1*, and *B2M*, Starkey et al., 2012), calcium homeostasis (*CALM1–3*), neurodegeneration (*CLU* and *PICALM*, Mengel-From et al., 2011), and oxidative stress (e.g., *PTGD2*, *CA11* and *SOD1*, Pareek et al., 2011). We carried out functional enrichment analysis using PANTHER version 7.0 (Mi et al., 2009; Thomas et al., 2003) on the group of highly expressed genes. Although many genes could not be classified, the most significant molecular pathways identified included the ubiquitin-proteasome pathway, synaptic transmission pathway, Huntington's disease, and PD (Supplementary Fig. 4). The overrepresentation of the PD pathway was mediated through genes encoding components of the ubiquitin-proteasome pathway (e.g., *PSMA1* and *PSMA2*), heat shock proteins (e.g., *HSPA2* and *HSPA5*), cell cycle components (e.g., *SEPT2*, *SEPT4*, and *SEPT5*), and synaptic genes (e.g., *SNCA*) among others. This shows that genes, for which mutations and/or variants that have been associated with PD, are components of cellular pathways that are highly expressed in the cortical and subcortical brain regions.

3.2. Extent of alternative promoter usage in brain transcriptome

We defined alternative TCs (ATCs) as those that mapped to the same gene but were separated by a distance of >300 bp. TCs that were unique for a single gene were defined as "dominant TC" (DTC). Compared with DTCs, ATCs were mostly noncanonical and at least 34% of them mapped to introns.

In our data, 60% of genes (10,205 of 16,888 expressed genes) used ATCs (mean 5, range of 2–356, Fig. 2). Most genes with ATC had at least 1 canonical TC. We noted that the number of ATC per gene was above 10 for 10% of the genes (Fig. 2). Because some of the genes were quite large, we used linear regression to model the number of ATC per gene (for genes with at least 16 ATCs- 5% of the genes with large number of ATCs) against gene size. We found a correlation of about 0.3 ($R = 0.28$, p value <2.2–16). This shows that gene length does not account to a large extent for the excess of ATC in genes. Outlier genes included *KCNIP4*, *PCDH9*, *CADM2*, *BAI3*, *NRG3*, *LSAMP*, *NRXN1*, *LRRTM4*, and *FGF14*, each with at least 100 ATCs. Functional enrichment analysis on genes with more than 16 ATCs (469 genes) showed an overrepresentation of glutamate receptor signaling and synaptic plasticity although most of the genes remained unclassified.

3.3. Regional differences in TC expression across the 5 brain regions

To identify signatures of gene expression across different brain regions, we sought CAGE clusters that were differentially expressed in one or more of the brain regions. We modeled the expression of the TCs using the number of counts and tested for significant differences in expression because of "regional effects" (see Section 2). We identified 7412 DETCs. Of these, 6037 were ATC of genes with a main canonical promoter. We identify neither any major differences in biotype between the differentially and nondifferentially expressed groups nor an excess of antisense TCs.

Fig. 3 presents the results of the hierarchical clustering for the 7412 DETCs. We identified 3 main branches: one connecting the striatal regions (caudate and putamen), one connecting the cortical regions (frontal and temporal), and a third that separated the hippocampal region from the other 2 groups. Fig. 3 also shows that the TCs were grouped into different clusters. We separated the

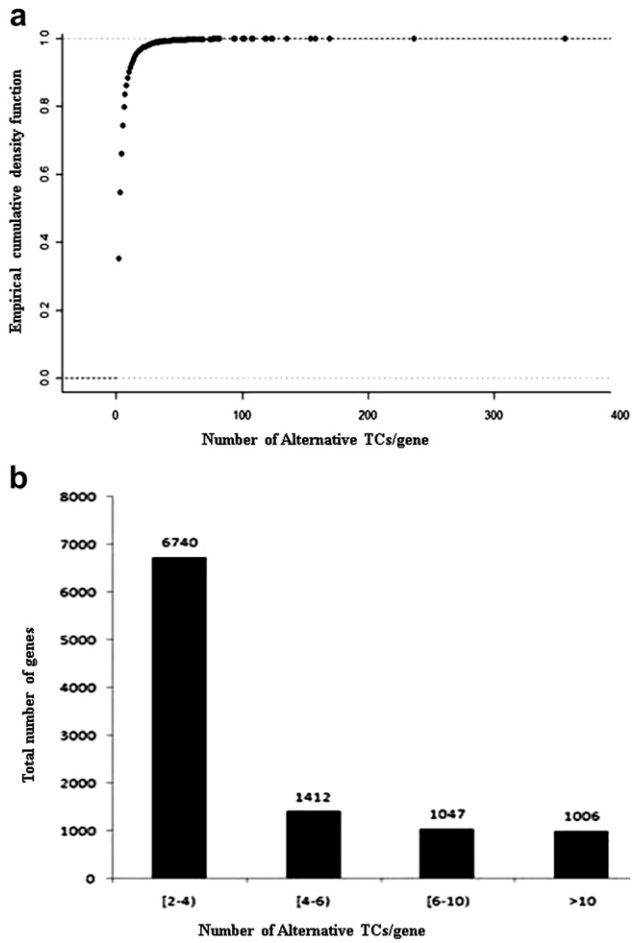

Fig. 2. Distribution of the number of alternative tag clusters (ATCs) per gene. (a) The empirical cumulative distribution (y-axis) of the number of ATCs per gene (x-axis) and (b) number of ATCs per bin category. The number of genes with 2 or more ATCs is shown at the top of every bin category.

DETCs into nonoverlapping modules (groups of TC that were differentially expressed in one or more regions) and identified 29 modules (Table 2). The largest module (M13) was characterized by small differences in expression across regions, and no region was clearly separated from the rest (Supplementary Fig. 5a). The other modules were characterized by more obvious differences in the average counts in 1 or 2 brain regions relative to the others (Supplementary Fig. 5b–d). These included M18 (lower expression in striatum vs. cortical regions and hippocampus), M4 (decreased expression in the caudate nucleus vs. the rest), M27 (lower expression in hippocampus), and M2 (increased expression in the cortex).

We evaluated whether specific signaling, metabolic, and disease pathways were enriched in the differentially expressed modules with at least 100 TCs. We used all the genes that were expressed in our data and that could be annotated in PANTHER version 7.0 as a reference set (Supplementary Table 4a shows the pathways that were significantly enriched in the reference group). Compared with the reference group, few pathways were enriched in the set of differentially expressed modules (Supplementary Fig. 6). The most significant pathway was the fibroblast growth factor (FGF) signaling pathway in M27 (lower expression in hippocampus) (p value <0.0005). Several genes from the *FGF* pathway were differentially expressed, including *FGF12*, *FGF14*, *RASA1*, *MAPK6*, *MAPK10*, *PPP2R2B*, and *PPA2*. All these genes had a main canonical TC that

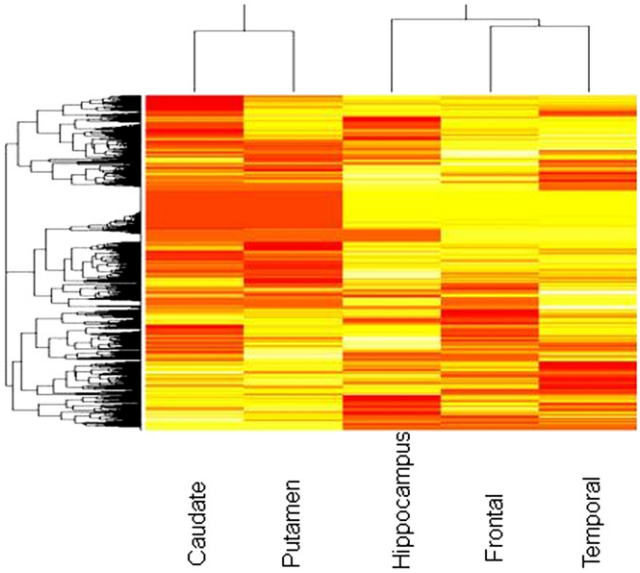

Fig. 3. Unsupervised clustering of differentially expressed tag clusters (DETC). The graph depicts the unsupervised clustering of the β coefficients of the factor "region" derived from the statistical analysis of differences in expression because of regional effects (see Section 2). The dendrogram at the top shows that basal ganglia cluster together and that frontal and temporal cortices cluster together. The dendrogram at the left of the graph was used to split the DETCs into functional modules (see Results).

was uniformly expressed across brain regions and an ATC showing reduced expression in hippocampus. Other significant pathways (p value <0.005) included platelet-derived growth factor signaling in M6 (lower expression in caudate compared with all other regions); synaptic trafficking in M2 (higher expression in cortex than in striatum and hippocampus) and M27 (lower expression in hippocampus); and glutamate receptor type I (metabotropic glutamate receptor group I [mGluRI]), *Wnt* signaling, and Huntington's disease pathways in M18 (lower expression in striatum compared with cortex and hippocampus). These significant pathways mediate many cell functions including proliferation, differentiation, and survival (Goldbeter and Pourquié, 2008; Moon et al., 2004; Peng et al., 2010). A list of enriched pathways per module and genes with TC in each of the pathways is presented in Supplementary Tables 4a and b, respectively.

3.4. Unexpected expression of neurodevelopmental transcription factors in aged brain

To investigate whether differential promoter usage across brain regions can be explained by differences in the manner in which they are regulated, we searched for transcription factors (TFs) that were differentially expressed across the 5 regions. We mapped all DETCs to a manually curated list of TFs (Vaquerizas et al., 2009). We identified 519 DETCs that mapped to 320 TF genes, although only 20% mapped to the promoter or 5′ UTR region (Supplementary Table 5). The DETF with the highest expression included those involved in neuronal postmitotic differentiation and laminar integrity in the cortex (e.g., *TBR1*, Bedogni et al., 2010, *NR2F1*, Naka et al., 2008, *NEUROD1*, *NEUROD2*, *BHLHE22*, and *MEF2C*) and neuronal plasticity (e.g., *NR4A1*) (Table 3 presents the top 20 most highly expressed TF per module). Most of the DETCs that mapped to TF were ATCs. One exception was a DTC that mapped to the promoter region of the *KLF5* gene and was differentially expressed in M27. *KLF5* has been shown to regulate survival and apoptosis through the regulation of MAPK kinase pathway. Other TFs that are module specific are presented in Supplementary Table 5.

To identify specific TFs that were coexpressed with (and possibly regulate) the DETCs, we screened proximal (−300/+100 bp) and distal (−1500/+500 bp) promoter sequences of all TCs for transcriptional factor binding sites (TFBS) using remote dependency models (see Supplementary data, Methods). Overall, we identified 3 classes of TFBS that were significantly overrepresented in the promoter regions of the DETC, namely, BPTF (FAC1), the TBX family, and CUX1 (CDP). These TFs stand out as regulators during neurodevelopment including dendritogenesis (CUX1) (Cubelos et al., 2010), cortical formation (Tbr1-TBX) (Bedogni et al., 2010), and neurite outgrowth (BPTF) (Rhodes et al., 2003). On the other hand, we found that 15 classes of TFBS were significantly underrepresented including *E2F*, *EGR* (KROX), the Sp family (*Sp1* and *Sp3*), *Elk1*, *ATF6*, *CREB1*, and *MYC*, and *KLF5*. These TFs are known to be involved in apoptosis (*E2F* and *KLF5*) and synaptic plasticity (*EGR1-2, CREB, KLF5*, and *Elk*).

We also screened every module separately. We identified significant over/under-representation of TFBS in 19 out of the 29 modules (Supplementary Table 6a and b). The *TBX* binding site was overrepresented in most of the modules, whereas the *BPTF* binding site was significantly overrepresented in M13 and M27. Other TFBS were overrepresented although they did not reach statistical significance (Supplementary Table 6a and b).

3.5. The extent of methylation in the brain transcriptome of aged individuals

DNA methylation at CpG nucleotides is another crucial mechanism for the regulation of gene expression (Jones, 2012). To investigate to what extent the patterns of expression in our data correlated with methylation, we analyzed methylation signatures in all 25 samples. After quality control and filtering, we obtained 551,178 MPs distributed and 95,715 of these were shared by at least 2 samples (of the 25 samples) and were used for downstream methylation analysis. We first assessed how many annotated genes from GENCODE were methylated and found that 73% of all methylation signals mapped within genes (Fig. 4), 43% to introns, 27% to exons, and 25% to promoter regions. We also looked at the proportion of methylation signals that occurred within CpG islands. We found that only 6% of methylated regions mapped within CpG islands. Of the promoters that mapped within CpG islands (45% of total), only 38% were methylated. Our data show that most of the methylated genomic regions occur in gene bodies and outside CpG islands (the list of MPs we used for the analysis is available on request).

3.5.1. Regional differences in methylation across the 5 brain regions

To identify DMP, specific for specific brain regions, we modeled the MPs using a linear model for regional effects, adjusting for both individual and possible methylation batch effects. Using this approach, we identified 13,423 DMPs, and of these 75.9% were mapped within gene bodies. Genes that were differentially methylated included *NRXN1*, *ITPR1*, *MADD*, *CNTNAP1*, *SRR*, *GABBR1*, *INPP5A*, *HTR1D*, *DLGAP1*, and *TIAM2*, which have been previously shown as methylated (Iwamoto et al., 2011) and that we found differentially methylated in frontal cortex.

We also compared the list of DMPs with MPs derived from Davies et al. (2012), where differences in methylation across several brain areas (mainly cortex and cerebellum) and blood were reported. We found that at least 39% of the DMPs overlapped with these from Davies et al. (2012). Moreover, several genes that we found differentially methylated showed also differences in methylation between cerebellum and cortex (e.g., *AACS*, *ADCY5*, *EPHB4*,

Table 2
Number of DE clusters identified for the DETCs

Module id	No. TCs	Caudate	Putamen	Hippocampus	Frontal	Temporal	Proportion of all DE TC
13	3190						0.43
18	1063						0.143
6	683						0.092
27	295						0.04
2	273						0.037
20	256						0.035
23	170						0.023
4	163						0.022
19	164						0.022
10	155						0.021
16	119						0.016
8	116						0.016
11	107						0.014
3	107						0.014
9	91						0.012
7	74						0.01
22	51						0.007
1	41						0.006
25	45						0.006
17	43						0.006
5	38						0.005
12	39						0.005
26	38						0.005
15	28						0.004
28	12						0.002
21	18						0.002
29	12						0.002
24	11						0.001
14	10						0.001
Total	**7412**						

Dark gray represents higher expression relative to other regions. Light gray represents lower expression relative to other regions. Black represents similar expression profile for all regions.
Key: DETCs, differentially expressed tag clusters.

GALNT9, and *GRM4*) and between brain and blood (e.g., *CCDC85A*, *PCDH9*, *PDE4D*, and *PPP2R2B*). This analysis shows that as much as 39% of methylated regions in brain (as identified by 2 different approaches) exhibit differences in their methylation profile in the brain regions we analyzed. The list of DMPs that we identified and that overlapped with MPs from Davies et al. (2012) is presented in Supplementary data, Data set 2).

3.5.2. Correlation between MPs and expression

To analyze the correlation between expression and methylation in our data, we first overlapped the genomic coordinates of both data sets considering promoter regions from −1500 to +500 bp relative to the most highly expressed TSS. We found that only 9% of all TCs overlapped with at least 1 MP. Overall, there was no significant correlation between methylation and expression (Spearman correlation: $r = -0.05$), most likely because of the large variation in the methylation of TCs with very low counts (Supplementary Fig. 8). We also analyzed the correlation between methylation and expression for protein-coding genes and non-coding genes separately (the number of ncRNA genes that overlapped with the MPs was too small to be analyzed independently) and did not observe any difference in their correlation coefficients (Spearman correlation of −0.06 and −0.07 for ncRNAs and protein-coding genes, respectively). Therefore, we tested for significant differences in expression because of "methylation effects" at individual TCs adjusting the expression for brain region and batch

Table 3
List of 20 most highly differentially expressed TF

TC ID	Start	End	TF	Module	Mean (geometric)
L3_chr2_+_161981068	161980893	161981527	*TBR1 (tbx family)*	13	28.718
L3_chr5_+_92946017	92945793	92946068	*NR2F1(COUP-tf1)*	13	6.658
L3_chr12_+_50731491	50731420	50731653	*NR4A1*	13	6.035
L3_chr7_+_39092007	39091721	39092121	*POU6F2*	13	5.520
L3_chr8_+_65655474	65655301	65655790	*BHLHE22*	13	5.035
L3_chr19_−_41561943	41561901	41561975	*ZFP14*	13	4.983
L3_chr5_−_88155431	88155327	88155565	*MEF2C*	13	4.965
L3_chr1_−_925340	925274	925452	*HES4*	13	4.738
L3_chr2_−_182253487	182253446	182253729	*NEUROD1*	13	4.271
L3_chr2_−_242205564	242205419	242205632	*THAP4*	13	3.994
L3_chr17_−_35017699	35017598	35017742	*NEUROD2*	13	3.946
L3_chr3_+_69871321	69871264	69871369	*MITF*	13	3.937
L3_chr13_+_72531139	72531098	72531259	*KLF5*	27	3.847
L3_chr4_+_146623601	146623337	146623645	*SMAD1*	13	3.750
L3_chr9_−_37455447	37455266	37455461	*ZBTB5*	13	3.745
L3_chr13_−_73606569	73606482	73606578	*KLF12*	13	3.587
L3_chr1_+_13977672	13977542	13977772	*PRDM2*	13	3.446
L3_chr19_+_60846825	60846530	60846828	*ZNF581*	13	3.399
L3_chr7_+_38984037	38983927	38984054	*POU6F2*	13	3.380
L3_chr2_+_45022343	45022302	45022747	*SIX3*	3	3.366

Key: TC, tag cluster; TF, transcription factor.

covariates. For this analysis, we only considered MPs that were present in at least 5 libraries. After correcting for multiple testing, we identified 312 TCs (5%) with differences in expression because of methylation effects. Of these, 34 TCs also exhibited differences in expression per region. Therefore, the differential expression because of regional effects we observed earlier was not driven by differences in methylation to a large extent. Genes with differences in expression per region because of methylation status included *CDK10*, *NRN1*, *PYCARD, TIMP3*, and *UCP2*. For these genes, promoter methylation has previously shown to regulate expression (Gloss et al., 2011; Konishi et al., 2011).

3.6. Effects of methylation on TF expression and TFBS

We compared the methylation status of differentially and non-DETFs. We did not identify any significant difference in the proportion of methylated TFs between the 2 groups (7% and 10% for differentially and non-DETFs, respectively). However, there was a significantly higher proportion of MPs mapping to the 3′ UTR regions in the DETFs (50% vs. 15%, Fisher $p = 0.0001$), whereas in the group of non-DETFs, most of the MPs mapped to the canonical promoter region (11% vs. 42%, Fisher $p = 0.0058$).

We also analyzed whether methylation could affect the expression of TCs by binding to their TFBS, presumably by modifying the spatial structure of binding sites (Choy et al., 2010). We screened the TFBS identified previously for overlaps with differentially MPs and found 304 TFBS in such locations (details of the statistical analysis are provided in Supplementary data, Methods). Out of all these TFBS, we only selected those, which overlap with differentially MPs showing a negative correlation between expression and methylation. Because of low number of high confident TFBS predictions made by RDM, we only identified a few TFs having several binding sites in such locations, namely, E2F group, Sp1:Sp3 complex, AP2alphaA, FAC1, and NHLH1 (for details, see Supplementary data, Methods and Table 7). This coincided with the underrepresentation of predicted TFBS for certain TFBS

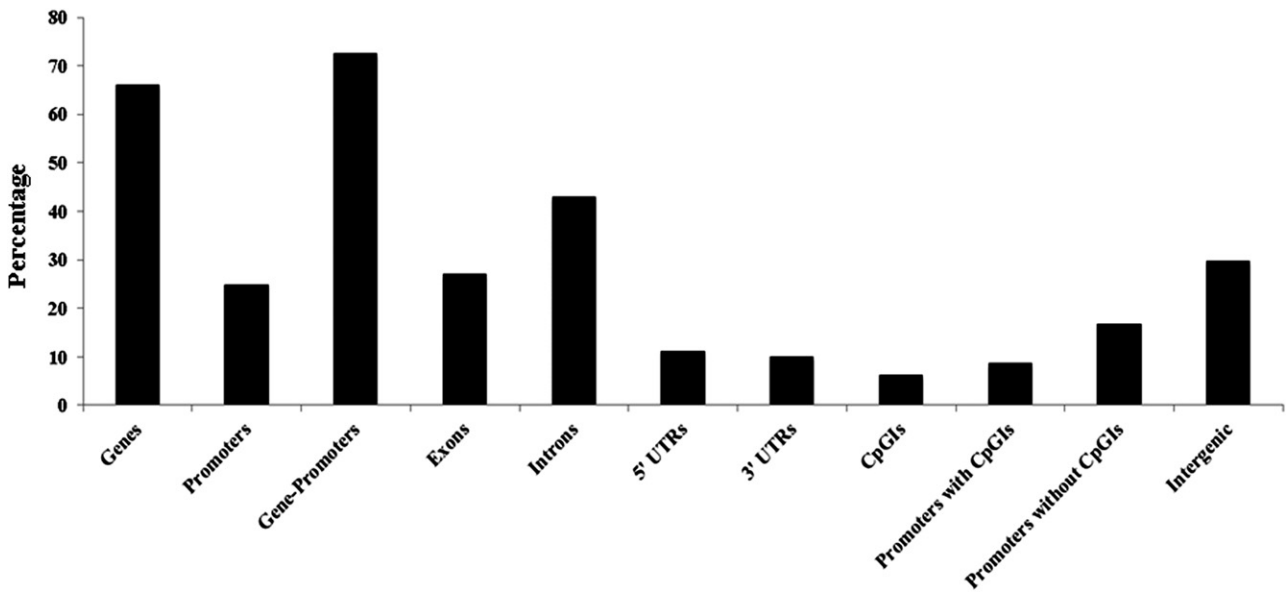

Fig. 4. Percentage of methylation peaks mapping to different gene regions, within and outside CpG islands.

including E2F and Sp1:Sp3 observed earlier (Supplementary Table 6a and b), suggesting that the corresponding TFs even being nondifferentially expressed may be involved in regulation of differential expression.

4. Discussion

In this study, we used CAGE in combination with massive parallel sequencing to profile transcription initiation across 5 different brain regions of aged, nondemented individuals and evaluated the extent of region specificity in alternative promoter usage and expression. At a sequencing depth of 1–2 million CAGE tags per library, we found that 40% of all GENCODE genes were expressed in brain. This estimate is probably conservative because it has been shown that deeper sequencing is needed to identify rare functional transcripts (Mercer et al., 2011). In addition, we annotated 6% of intergenic TCs to 559 lncRNAs that had previously only been predicted in silico.

We found that 77% of the genes with canonical TCs in our data set overlap with another brain transcriptome data set derived from RNA-Seq methodology (Ramskold et al., 2009). Comparing the 2 data sets reveals that CAGE detects more ncRNA transcripts (e.g., lncRNAs and pseudogenes) whereas the proportion of protein-coding genes was higher with RNA-Seq. These differences could be the result of differences in sequencing depth or due to marked differences in the experimental design of both approaches. Indeed, although CAGE and RNA-Seq can be used to quantify the amount of gene expression and that there is a high correlation of gene expression between these 2 approaches (0.57, see Dong et al., 2012), RNA-Seq libraries are commonly enriched for poly A+ transcripts (Mortazavi et al., 2008) of which protein-coding genes are an abundant class. In contrast, CAGE method captures capped RNA transcripts of both poly A+ and poly A− classes (Carninci, 2007). This also may explain why some genes that appeared highly expressed in brain in the RNA-Seq data set were not identified with CAGE including mitochondrial and ribosomal genes because they are uncapped and, therefore, not well covered by the CAGE approach.

Recent studies show that ncRNAs regulate gene expression in brain and play a role in the development and in the onset of neurologic diseases (Schonrock et al., 2011). Most research has focused on deciphering the functional role of lncRNAs and miRNAs, but other classes of ncRNAs may also be important. We found that more than 4.7% of the total RNA pool (and 24% of the ncRNA) consisted of annotated pseudogenes. The contribution of this ncRNA class to the transcriptome is currently unknown, with estimates ranging from 5% (Frith et al., 2006), which is consistent with our data, to 20% (Pink et al., 2011). Although the functional impact of ncRNA classes was not assessed in this study, our findings demonstrate that pseudogene expression is a pervasive feature of the transcriptome in aged brain.

We found expression patterns consistent with aging, including high expression of *GPAFP* (Starkey et al., 2012) and *SPARCL1*, which are markers of gliosis, and high expression of genes involved in protection against oxidative stress and amyloid aggregation. This group includes *CLU*, the gene for clusterin, an extracellular chaperone that maintains stressed proteins in a soluble state, thereby preventing their precipitation (Poon et al., 2002). Clusterin colocalizes with amyloid plaques and neurofibrillary tangles, and it has been suggested that it protects neurons from aggregate-induced damage (Yerbury et al., 2007). The ubiquitin-proteosome pathway was overrepresented in the group of highly expressed genes. This pathway has been shown to be downregulated in disorders such as AD and PD (Dennissen et al., 2012), and this decrease correlates with a failure of neurons to remove toxic protein aggregates. In this regard, it is important to stress that despite some pathologic findings consistent with aging, none of the 7 donors used for this study showed any overt AD or PD pathology (Braak tangle stages $\leq$3 and Braak α-synuclein stage 0–IV; Supplementary Table 1). These results suggest that increased expression of genes involved in the ubiquitin-proteosome pathway and neuroprotection (e.g., *CLU*) may help to protect against overt protein aggregation in aged healthy individuals.

It has been recently shown that alternative promoter usage and alternative splicing can explain differences in gene expression across brain regions (Pal et al., 2011; Tollervey et al., 2011). Our data support the role of alternative promoters in causing expression differences between brain regions. We found that 81% of the DETCs were putative alternative TSS of genes with a main promoter that was similarly expressed in all the regions analyzed. This shows that the major transcripts were more often uniformly expressed whereas alternative transcripts were more likely to be region specific. Alternative promoters can alter the expression of a main transcript by competing for the cell's transcription machinery (Davuluri et al., 2008) or by antagonizing the effects of the main transcript (Tschan et al., 2003). For example, we found a DETC in M18 (Supplementary Table 5) mapping to the promoter region of a short isoform of *DMTF1*, which has been shown to antagonize the effects of the main *DMTF1* transcript in myeloid lines (Tschan et al., 2003). Whether the expression of the shorter isoform leads to the same changes observed in other cells cannot be ascertained here, but it suggests an interesting mechanism by which alternative promoter usage might lead to differences in expression.

In our data, most of the ATCs that were differentially expressed were located in noncanonical gene regions (Fig. 1a), particularly in introns. Although there is evidence that CAGE tags can also mark post-transcriptional events (Mercer et al., 2010), we provide several lines of evidence indicating that a proportion of transcription is initiated from noncanonical gene regions. First, we only included CAGE clusters present in at least 2 biological replicas, which makes it unlikely that a tag identified twice is the result of an artifact. Second, we found that at least one-third of noncanonical TCs overlapped with other signatures of promoter activity derived from H3K4me3 histone marks (data not shown). In addition, we confirmed with RACE the existence of capped products for 4 putative alternative TSSs in the *CNP*, *RTN4*, *NRG3*, and *AUTS2* genes (Supplementary data, Results), which may represent novel isoforms for those genes. Indeed, we confirmed experimentally the presence of an alternative TSS in the intronic region of *AUTS2*, which is associated with a shorter transcript that was previously only in silico predicted. Our results indicate that at least one-third of alternative TSS map to intronic gene regions.

Several growth factor signaling pathways have been implicated in the alterations that render neuronal cell populations susceptible to neurodegeneration. Our data showed that the *FGF*, epidermal growth factor (*EGF*), insulin growth factor (*IGF*), and platelet-derived growth factor pathways were overrepresented in several differentially expressed modules (Supplementary Fig. 5 and Table 4a). Common to these pathways is the mitogen-activated protein kinase (MAPK) cascade that has a broad range of effects on cellular function including survival and differentiation (Thomas and Huganir, 2004). The FGF signaling pathway was the most significantly overrepresented pathway in module M27, where a reduced expression in hippocampus was observed. The hippocampal region is a primary target of the neurodegenerative changes that lead to cognitive impartment and AD. Several mechanisms have been suggested to lead to hippocampal dysfunction, including decreased neuronal plasticity and increased calcium toxicity. The FGF pathway can influence neural plasticity through several mechanisms including MAPK/ERK activation (Thomas and Huganir, 2004), and

its expression was reduced in the hippocampus relative to other regions. These findings suggest that the FGF pathway could be an important target for pharmacologic treatments to combat neurodegeneration.

The caudate and putamen regions (striatum), which are components of the cortical-subcortical circuits of motor functions, are particularly susceptible to neurodegeneration in disorders such as Huntington's disease and PD (DeLong and Wichmann, 2007). Interestingly, functional enrichment analysis based on several DETCs showed that genes encoding components of the *Wnt* signaling pathway and the mGluRI were significantly overrepresented in the modules where coexpression in the striatal regions was observed (M18; Table 2). Both *Wnt* signaling and mGluRI have been implicated in the development or progression of PD (Johnson et al., 2009; L'Episcopo et al., 2011). Moreover, mGluRI modulates neurotransmission throughout the basal ganglia, and its deregulation can contribute to neuronal damage (Johnson et al., 2009). Our results suggest that in the absence of a clear genetic risk, pathways other than those associated with classical mutations are important determinants of the regional vulnerability in the aging brain.

We investigated whether differences in expression could be attributed to differential TF expression. We found that 7% of TFs were differentially expressed, and many of these have been shown to be involved in the neurodevelopment, which is unexpected given that neurons are postmitotic cells. The TFBS analysis also showed an overrepresentation binding sites for TFs involved in neurodevelopment. There are few explanations for this finding including a bias in the literature toward functional annotation of neurodevelopmental TFs. Another plausible explanation is that, as the brain ages, these genes may become derepressed because of, for example, damage in their promoter regions. Although we did not find decreased methylation in the group of DETFs, we found decreased methylation in the promoter region of this group and increased methylation in the 3′ UTRs. Methylation marks at both ends of transcriptional units could affect the expression of the group of DETFs (Jones, 2012).

Our analysis of methylation indicated that most of the methylation signals in our samples mapped to gene bodies and outside CpG islands. This is consistent with recent evidence that in brain most methylation signals occur within gene bodies, most likely in association with alternative promoters (Maunakea et al., 2010). However, we did not find an overall correlation between methylation and TC expression. Several factors could account for the lack of correlation. For example, batch effects were evident in the CAGE data set. In addition, only 9% of the methylated regions colocalized with a TC, which means that most of the expression in our data remained uninvestigated. The lack of overlap between the MPs and the CAGE clusters could also be because of the fact that the arrays we used to profile methylation were biased toward annotated promoters and CpG islands, whereas our CAGE clusters mapped to a large extent to noncanonical regions. Last, as a result of the small sample size, most of MPs were identified in less than 5 samples and were removed from the statistical analyses. Despite this drawback, we identified several gene-associated TCs that were affected by methylation, some of which were already documented (Iwamoto et al., 2011).

Our study is far from being comprehensive because of our small sample size and the limited number of brain regions analyzed. In addition, because of the diverse cellular composition of the brain, one might argue that the expression we observed is not exclusive to neuronal populations, although neurons and glia cells represent most of the cellular pool in human brain. A separate issue is that most of our bioinformatics analysis used public databases, which are still incomplete. For example, many protein-coding genes that we found differentially expressed could not be assigned to any functional pathway because of a lack of annotation. Therefore, inferences about functional pathways are based on a limited number of genes. Nonetheless, our data set provides an important addition to existing data on spatial expression patterns in brain.

In summary, our study shows that despite the absence of neuropathologic hallmarks of neurodegenerative disease, genetic signatures related to neurodegeneration were already present in brain regions that are highly vulnerable to neurologic disorders. We showed that differences in transcription initiation and hence gene expression between brain regions are partly explained by alternative promoter usage and that specific signaling pathways are affected by the differential patterns in gene expression that we observed. Our data are a starting point to investigate regional susceptibility to brain aging and neurodegeneration.

Disclosure statement

The authors declare no conflicts of interest.

Acknowledgements

The authors thank the Netherlands Brain Bank (Amsterdam, the Netherlands), especially Michiel Kooreman, for providing excellent postmortem human brain tissue and are grateful to all controls who donated their brains, K. Lo (Roche) for providing with an R script to identify differentially methylated regions, and Aad W. van der Vaart and Wessel N. van Wieringen for useful discussions on the statistical analysis of differential expression. G.G.R.L. is partly supported by the Center for Medical Systems Biology, established by the Netherlands Genomics Initiative/Netherlands Organization for Scientific Research. M.F. is funded by Portuguese Foundation for Science and Technology (scholarship reference SFRH/BD/33536/2008). J.S.S. is funded by Hersenstichting Nederland Fellowship project B08.03 and the Neuroscience Campus Amsterdam.

Appendix A. Supplementary data

Supplementary data associated with this article can be found, in the online version, at http://dx.doi.org/10.1016/j.neurobiolaging.2013.01.005.

References

Abdolmaleky, H.M., K-h, Cheng, Russo, A., Smith, C.L., Faraone, S.V., Wilcox, M., Shafa, R., Glatt, S.J., Nguyen, G., Ponte, J.F., Thiagalingam, S., Tsuang, M.T., 2005. Hypermethylation of the reelin (RELN) promoter in the brain of schizophrenic patients: a preliminary report. American Journal of Medical Genetics Part B: Neuropsychiatric Genetics 134B, 60–66.

Alafuzoff, I., Arzberger, T., Al-Sarraj, S., Bodi, I., Bogdanovic, N., Braak, H., Bugiani, O., Del-Tredici, K., Ferrer, I., Gelpi, E., Giaccone, G., Graeber, M.B., Ince, P., Kamphorst, W., King, A., Korkolopoulou, P., Kovács, G.G., Larionov, S., Meyronet, D., Monoranu, C., Parchi, P., Patsouris, E., Roggendorf, W., Seilhean, D., Tagliavini, F., Stadelmann, C., Streichenberger, N., Thal, D.R., Wharton, S.B., Kretzschmar, H., 2008. Staging of neurofibrillary pathology in Alzheimer's Disease: a study of the BrainNet Europe Consortium. Brain Pathology 18, 484–496.

Alafuzoff, I., Ince, P.G., Arzberger, T., Al-Sarraj, S., Bell, J., Bodi, I., Bogdanovic, N., Bugiani, O., Ferrer, I., Gelpi, E., Gentleman, S., Giaccone, G., Ironside, J.W., Kavantzas, N., King, A., Korkolopoulou, P., Kovacs, G.G., Meyronet, D., Monoranu, C., Parchi, P., Parkkinen, L., Patsouris, E., Roggendorf, W., Rozemuller, A., Stadelmann-Nessler, C., Streichenberger, N., Thal, D.R., Kretzschmar, H., 2009a. Staging/typing of Lewy body related alpha-synuclein pathology: a study of the BrainNet Europe Consortium. Acta neuropathologica. 117, 635–652.

Alafuzoff, I., Thal, D.R., Arzberger, T., Bogdanovic, N., Al-Sarraj, S., Bodi, I., Boluda, S., Bugiani, O., Duyckaerts, C., Gelpi, E., Gentleman, S., Giaccone, G., Graeber, M., Hortobagyi, T., Hoftberger, R., Ince, P., Ironside, J.W., Kavantzas, N., King, A., Korkolopoulou, P., Kovacs, G.G., Meyronet, D., Monoranu, C., Nilsson, T., Parchi, P., Patsouris, E., Pikkarainen, M., Revesz, T., Rozemuller, A., Seilhean, D.,

Schulz-Schaeffer, W., Streichenberger, N., Wharton, S.B., Kretzschmar, H., 2009b. Assessment of beta-amyloid deposits in human brain: a study of the BrainNet Europe Consortium. Acta neuropathologica. 117, 309–320.

Bandopadhyay, R., Kingsbury, A.E., Cookson, M.R., Reid, A.R., Evans, I.M., Hope, A.D., Pittman, A.M., Lashley, T., Canet-Aviles, R., Miller, D.W., McLendon, C., Strand, C., Leonard, A.J., Abou-Sleiman, P.M., Healy, D.G., Ariga, H., Wood, N.W., de Silva, R., Revesz, T., Hardy, J.A., Lees, A.J., 2004. The expression of DJ-1(PARK7) in normal human CNS and idiopathic Parkinson's disease. Brain 127, 420–430.

Bedogni, F., Hodge, R.D., Elsen, G.E., Nelson, B.R., Daza, R.A.M., Beyer, R.P., Bammler, T.K., Rubenstein, J.L.R., Hevner, R.F., 2010. Tbr1 regulates regional and laminar identity of postmitotic neurons in developing neocortex. Proc. Natl. Acad. Sci. U S A 107, 13129–13134.

Braak, H., Bohl, J.R., Muller, C.M., Rub, U., de Vos, R.A., Del Tredici, K., 2006. Stanley Fahn Lecture 2005: the staging procedure for the inclusion body pathology associated with sporadic Parkinson's disease reconsidered. Mov. Disord. 21, 2042–2051.

Carninci, P., 2007. Constructing the landscape of the mammalian transcriptome. J .Exp. Biol. 210, 1497–1506.

Carninci, P., Kasukawa, T., Katayama, S., Gough, J., Frith, M.C., Maeda, N., Oyama, R., Ravasi, T., Lenhard, B., Wells, C., Kodzius, R., Shimokawa, K., Bajic, V.B., Brenner, S.E., Batalov, S., Forrest, A.R., Zavolan, M., Davis, M.J., Wilming, L.G., Aidinis, V., Allen, J.E., Ambesi-Impiombato, A., Apweiler, R., Aturaliya, R.N., Bailey, T.L., Bansal, M., Baxter, L., Beisel, K.W., Bersano, T., Bono, H., Chalk, A.M., Chiu, K.P., Choudhary, V., Christoffels, A., Clutterbuck, D.R., Crowe, M.L., Dalla, E., Dalrymple, B.P., de Bono, B., Della Gatta, G., di Bernardo, D., Down, T., Engstrom, P., Fagiolini, M., Faulkner, G., Fletcher, C.F., Fukushima, T., Furuno, M., Futaki, S., Gariboldi, M., Georgii-Hemming, P., Gingeras, T.R., Gojobori, T., Green, R.E., Gustincich, S., Harbers, M., Hayashi, Y., Hensch, T.K., Hirokawa, N., Hill, D., Huminiecki, L., Iacono, M., Ikeo, K., Iwama, A., Ishikawa, T., Jakt, M., Kanapin, A., Katoh, M., Kawasawa, Y., Kelso, J., Kitamura, H., Kitano, H., Kollias, G., Krishnan, S.P., Kruger, A., Kummerfeld, S.K., Kurochkin, I.V., Lareau, L.F., Lazarevic, D., Lipovich, L., Liu, J., Liuni, S., McWilliam, S., Madan Babu, M., Madera, M., Marchionni, L., Matsuda, H., Matsuzawa, S., Miki, H., Mignone, F., Miyake, S., Morris, K., Mottagui-Tabar, S., Mulder, N., Nakano, N., Nakauchi, H., Ng, P., Nilsson, R., Nishiguchi, S., Nishikawa, S., Nori, F., Ohara, O., Okazaki, Y., Orlando, V., Pang, K.C., Pavan, W.J., Pavesi, G., Pesole, G., Petrovsky, N., Piazza, S., Reed, J., Reid, J.F., Ring, B.Z., Ringwald, M., Rost, B., Ruan, Y., Salzberg, S.L., Sandelin, A., Schneider, C., Schonbach, C., Sekiguchi, K., Semple, C.A., Seno, S., Sessa, L., Sheng, Y., Shibata, Y., Shimada, H., Shimada, K., Silva, D., Sinclair, B., Sperling, S., Stupka, E., Sugiura, K., Sultana, R., Takenaka, Y., Taki, K., Tammoja, K., Tan, S.L., Tang, S., Taylor, M.S., Tegner, J., Teichmann, S.A., Ueda, H.R., van Nimwegen, E., Verardo, R., Wei, C.L., Yagi, K., Yamanishi, H., Zabarovsky, E., Zhu, S., Zimmer, A., Hide, W., Bult, C., Grimmond, S.M., Teasdale, R.D., Liu, E.T., Brusic, V., Quackenbush, J., Wahlestedt, C., Mattick, J.S., Hume, D.A., Kai, C., Sasaki, D., Tomaru, Y., Fukuda, S., Kanamori-Katayama, M., Suzuki, M., Aoki, J., Arakawa, T., Iida, J., Imamura, K., Itoh, M., Kato, T., Kawaji, H., Kawagashira, N., Kawashima, T., Kojima, M., Kondo, S., Konno, H., Nakano, K., Ninomiya, N., Nishio, T., Okada, M., Plessy, C., Shibata, K., Shiraki, T., Suzuki, S., Tagami, M., Waki, K., Watahiki, A., Okamura-Oho, Y., Suzuki, H., Kawai, J., Hayashizaki, Y., 2005. The transcriptional landscape of the mammalian genome. Science 309, 1559–1563.

Carninci, P., Sandelin, A., Lenhard, B., Katayama, S., Shimokawa, K., Ponjavic, J., Semple, C.A., Taylor, M.S., Engstrom, P.G., Frith, M.C., Forrest, A.R., Alkema, W.B., Tan, S.L., Plessy, C., Kodzius, R., Ravasi, T., Kasukawa, T., Fukuda, S., Kanamori-Katayama, M., Kitazume, Y., Kawaji, H., Kai, C., Nakamura, M., Konno, H., Nakano, K., Mottagui-Tabar, S., Arner, P., Chesi, A., Gustincich, S., Persichetti, F., Suzuki, H., Grimmond, S.M., Wells, C.A., Orlando, V., Wahlestedt, C., Liu, E.T., Harbers, M., Kawai, J., Bajic, V.B., Hume, D.A., Hayashizaki, Y., 2006. Genome-wide analysis of mammalian promoter architecture and evolution. Nature genetics 38, 626–635.

Choy, M.-K., Movassagh, M., Goh, H.-G., Bennett, M., Down, T., Foo, R., 2010. Genome-wide conserved consensus transcription factor binding motifs are hyper-methylated. BMC Genomics 11, 519–529.

Cubelos, B., Sebastián-Serrano, A., Beccari, L., Calcagnotto, M.E., Cisneros, E., Kim, S., Dopazo, A., Alvarez-Dolado, M., Redondo, J.M., Bovolenta, P., Walsh, C.A., Nieto, M., 2010. Cux1 and Cux2 regulate dendritic branching, spine morphology, and synapses of the upper layer neurons of the cortex. Neuron 66, 523–535.

Davies, M.N., Volta, M., Pidsley, R., Lunnon, K., Dixit, A., Lovestone, S., Coarfa, C., Harris, R.A., Milosavljevic, A., Troakes, C., Al-Sarraj, S., Dobson, R., Schalkwyk, L.C., Mill, J., 2012. Functional annotation of the human brain methylome identifies tissue- specific epigenetic variation across brain and blood. Genome Biol. 13, R43.

Davuluri, R.V., Suzuki, Y., Sugano, S., Plass, C., Huang, T.H., 2008. The functional consequences of alternative promoter use in mammalian genomes. Trends Genet. 24, 167–177.

De Hoon, M.J., Bertin, N., Chalk, A.M., 2010. Using CAGE data for quantitative expression. In: Carninci, P. (Ed.), Cap Analysis Gene Expression (CAGE): The Science of decoding Gene Transcription. Pan Standford Publishing Pte. Ltd, Yokohama, pp. 101–121.

DeLong, M.R., Wichmann, T., 2007. Circuits and circuit disorders of the basal ganglia. Arch Neurol. 64, 20–24.

Dennissen, F.J., Kholod, N., van Leeuwen, F.W., 2012. The ubiquitin proteasome system in neurodegenerative diseases: culprit, accomplice or victim? Progress in neurobiology 96, 190–207.

Dong, X., Greven, M.C., Kundaje, A., Djebali, S., Brown, J.B., Cheng, C., Gingeras, T.R., Gerstein, M., Guigó, R., Birney, E., Weng, Z., 2012. Modeling gene expression using chromatin features in various cellular contexts. Genome Biol. 13, R53.

Double, K.L., Halliday, G.M., Kril, J.J., Harasty, J.A., Cullen, K., Brooks, W.S., Creasey, H., Broe, G.A., 1996. Topography of brain atrophy during normal aging and Alzheimer's disease. Neurobiology of aging 17, 513–521.

Double, K.L., Reyes, S., Werry, E.L., Halliday, G.M., 2010. Selective cell death in neurodegeneration: why are some neurons spared in vulnerable regions? Progress in neurobiology 92, 316–329.

Faulkner, G.J., Forrest, A.R., Chalk, A.M., Schroder, K., Hayashizaki, Y., Carninci, P., Hume, D.A., Grimmond, S.M., 2008. A rescue strategy for multimapping short sequence tags refines surveys of transcriptional activity by CAGE. Genomics 91, 281–288.

Frith, M.C., Wilming, L.G., Forrest, A., Kawaji, H., Tan, S.L., Wahlestedt, C., Bajic, V.B., Kai, C., Kawai, J., Carninci, P., Hayashizaki, Y., Bailey, T.L., Huminiecki, L., 2006. Pseudo-messenger RNA: phantoms of the Transcriptome. PLoS genetics 2, e23.

Fujita, P.A., Rhead, B., Zweig, A.S., Hinrichs, A.S., Karolchik, D., Cline, M.S., Goldman, M., Barber, G.P., Clawson, H., Coelho, A., Diekhans, M., Dreszer, T.R., Giardine, B.M., Harte, R.A., Hillman-Jackson, J., Hsu, F., Kirkup, V., Kuhn, R.M., Learned, K., Li, C.H., Meyer, L.R., Pohl, A., Raney, B.J., Rosenbloom, K.R., Smith, K.E., Haussler, D., Kent, W.J., 2011. The UCSC Genome Browser database: update 2011. Nucleic Acids Res. 39, D876–D882.

Gloss, B.S., Patterson, K.I., Barton, C.A., Gonzalez, M., Scurry, J.P., Hacker, N.F., Sutherland, R.L., O'Brien, P.M., Clark, S.J., 2011. Integrative genome-wide expression and promoter DNA methylation profiling identifies a potential novel panel of ovarian cancer epigenetic biomarkers. Cancer Letters 318, 76–85.

Goldbeter, A., Pourquié, O., 2008. Modeling the segmentation clock as a network of coupled oscillations in the Notch, Wnt and FGF signaling pathways. Journal of Theoretical Biology 252, 574–585.

Hardy, J., Selkoe, D.J., 2002. The amyloid hypothesis of Alzheimer's Disease: progress and problems on the road to therapeutics. Science 297, 353–356.

Harrow, J., Denoeud, F., Frankish, A., Reymond, A., Chen, C.-K., Chrast, J., Lagarde, J., Gilbert, J., Storey, R., Swarbreck, D., Rossier, C., Ucla, C., Hubbard, T., Antonarakis, S., Guigo, R., 2006. GENCODE: producing a reference annotation for ENCODE. Genome Biol. 7 (Suppl 1), S4.1–S4.9.

Iwamoto, K., Bundo, M., Ueda, J., Oldham, M.C., Ukai, W., Hashimoto, E., Saito, T., Geschwind, D.H., Kato, T., 2011. Neurons show distinctive DNA methylation profile and higher interindividual variations compared with non-neurons. Genome Res. 21, 688–696.

Jia, H., Osak, M., Bogu, G.K., Stanton, L.W., Johnson, R., Lipovich, L., 2010. Genome-wide computational identification and manual annotation of human long noncoding RNA genes. RNA 16, 1478–1487.

Joachim, C.L., Mori, H., Selkoe, D.J., 1989. Amyloid beta-protein deposition in tissues other than brain in Alzheimer's disease. Nature 341, 226–230.

Johnson, K.A., Conn, P.J., Niswender, C.M., 2009. Glutamate receptors as therapeutic targets for Parkinson's disease. CNS & neurological disorders drug targets 8, 475–491.

Johnson, M.B., Kawasawa, Y.I., Mason, C.E., Krsnik, Z., Coppola, G., Bogdanovic, D., Geschwind, D.H., Mane, S.M., State, M.W., Sestan, N., 2009. Functional and evolutionary insights into human brain development through global transcriptome analysis. Neuron 62, 494–509.

Jones, P.A., 2012. Functions of DNA methylation: islands, start sites, gene bodies and beyond. Nature reviews 13, 484–492.

Kang, H.J., Kawasawa, Y.I., Cheng, F., Zhu, Y., Xu, X., Li, M., Sousa, A.M.M., Pletikos, M., Meyer, K.A., Sedmak, G., Guennel, T., Shin, Y., Johnson, M.B., Krsnik, Z., Mayer, S., Fertuzinhos, S., Umlauf, S., Lisgo, S.N., Vortmeyer, A., Weinberger, D.R., Mane, S., Hyde, T.M., Huttner, A., Reimers, M., Kleinman, J.E., Sestan, N., 2011. Spatio-temporal transcriptome of the human brain. Nature 478, 483–489.

Khaitovich, P., Muetzel, B., She, X., Lachmann, M., Hellmann, I., Dietzsch, J., Steigele, S., Do, H.H., Weiss, G., Enard, W., Heissig, F., Arendt, T., Nieselt-Struwe, K., Eichler, E.E., Paabo, S., 2004. Regional patterns of gene expression in human and chimpanzee brains. Genome research 14, 1462–1473.

Kodzius, R., Kojima, M., Nishiyori, H., Nakamura, M., Fukuda, S., Tagami, M., Sasaki, D., Imamura, K., Kai, C., Harbers, M., Hayashizaki, Y., Carninci, P., 2006. CAGE: cap analysis of gene expression. Nat. Meth. 3, 211–222.

Konishi, K., Watanabe, Y., Shen, L., Guo, Y., Castoro, R.J., Kondo, K., Chung, W., Ahmed, S., Jelinek, J., Boumber, Y.A., Estecio, M.R., Maegawa, S., Kondo, Y., Itoh, F., Imawari, M., Hamilton, S.R., Issa J-, P.J., 2011. DNA methylation profiles of primary colorectal carcinoma and matched liver metastasis. PloS one 6, e27889.

Konopka, G., Geschwind, D.H., 2010. Human brain evolution: harnessing the genomics (r)evolution to link genes, cognition, and behavior. Neuron 68, 231–244.

L'episcopo, F., Serapide, M.F., Tirolo, C., Testa, N., Caniglia, S., Morale, M.C., Pluchino, S., Marchetti, B., 2011. Wnt1 regulated Frizzled-1/beta-Catenin signaling pathway as a candidate regulatory circuit controlling mesencephalic dopaminergic neuron-astrocyte crosstalk: therapeutical relevance for neuron survival and neuroprotection. Molecular Degeneration 6, 49–78.

Lassmann, T., Hayashizaki, Y., Daub, C.O., 2009. TagDust–a program to eliminate artifacts from next generation sequencing data. Bioinformatics 25, 2839–2840.

Maunakea, A.K., Nagarajan, R.P., Bilenky, M., Ballinger, T.J., D'Souza, C., Fouse, S.D., Johnson, B.E., Hong, C., Nielsen, C., Zhao, Y., Turecki, G., Delaney, A., Varhol, R., Thiessen, N., Shchors, K., Heine, V.M., Rowitch, D.H., Xing, X., Fiore, C., Schillebeeckx, M., Jones, S.J.M., Haussler, D., Marra, M.A., Hirst, M., Wang, T., Costello, J.F., 2010. Conserved role of intragenic DNA methylation in regulating alternative promoters. Nature 466, 253–257.

Mengel-From, J., Christensen, K., McGue, M., Christiansen, L., 2011. Genetic variations in the CLU and PICALM genes are associated with cognitive function in the oldest old. Neurobiology of aging 32, 554e7–11.

Mercer, T.R., Dinger, M.E., Bracken, C.P., Kolle, G., Szubert, J.M., Korbie, D.J., Askarian-Amiri, M.E., Gardiner, B.B., Goodall, G.J., Grimmond, S.M., Mattick, J.S., 2010. Regulated post-transcriptional RNA cleavage diversifies the eukaryotic transcriptome. Genome Res. 20, 1639–1650.

Mercer, T.R., Gerhardt, D.J., Dinger, M.E., Crawford, J., Trapnell, C., Jeddeloh, J.A., Mattick, J.S., Rinn, J.L., 2011. Targeted RNA sequencing reveals the deep complexity of the human transcriptome. Nat. Biotech. 30, 99–104.

Mi, H., Dong, Q., Muruganujan, A., Gaudet, P., Lewis, S., Thomas, P.D., 2009. PANTHER version 7: improved phylogenetic trees, orthologs and collaboration with the Gene Ontology Consortium. Nucleic Acids Res. 38. D204–DD10.

Miller, C.A., Sweatt, J.D., 2007. Covalent modification of DNA regulates memory formation. Neuron 53, 857–869.

Moon, R.T., Kohn, A.D., Ferrari, G.V.D., Kaykas, A., 2004. WNT and [beta]-catenin signalling: diseases and therapies. Nature reviews 5, 691–701.

Mortazavi, A., Williams, B.A., McCue, K., Schaeffer, L., Wold, B., 2008. Mapping and quantifying mammalian transcriptomes by RNASeq. Nat. Methods 5, 621–628.v.

Naka, H., Nakamura, S., Shimazaki, T., Okano, H., 2008. Requirement for COUP-TFI and II in the temporal specification of neural stem cells in CNS development. Nat. Neurosci. 11, 1014–1023.

Pal, S., Gupta, R., Kim, H., Wickramasinghe, P., Baubet, V., Showe, L.C., Dahmane, N., Davuluri, R.V., 2011. Alternative transcription exceeds alternative splicing in generating the transcriptome diversity of cerebellar development. Genome Res. 21, 1260–1272.

Pareek, T.K., Belkadi, A., Kesavapany, S., Zaremba, A., Loh, S.L., Bai, L., Cohen, M.L., Meyer, C., Liby, K.T., Miller, R.H., Sporn, M.B., Letterio, J.J., 2011. Triterpenoid modulation of IL-17 and Nrf-2 expression ameliorates neuroinflammation and promotes remyelination in autoimmune encephalomyelitis. Sci. Rep. 201, 1–11.

Peng, F., Yao, H., Bai, X., Zhu, X., Reiner, B.C., Beazely, M., Funa, K., Xiong, H., Buch, S., 2010. Platelet-derived growth factor-mediated induction of the synaptic plasticity gene Arc/Arg3.1. J. Biol. Chem. 285, 21615–21624.

Pink, R.C., Wicks, K., Caley, D.P., Punch, E.K., Jacobs, L., Francisco Carter, D.R., 2011. Pseudogenes: pseudo-functional or key regulators in health and disease? RNA 17, 792–798.

Poon, S., Treweek, T.M., Wilson, M.R., Easterbrook-Smith, S.B., Carver, J.A., 2002. Clusterin is an extracellular chaperone that specifically interacts with slowly aggregating proteins on their off-folding pathway. FEBS Lett. 513, 259–266.

Purcell, S., Neale, B., Todd-Brown, K., Thomas, L., Ferreira, M.A., Bender, D., Maller, J., Sklar, P., de Bakker, P.I., Daly, M.J., Sham, P.C., 2007. PLINK: a tool set for whole-genome association and populationbased linkage analyses. Am. J. Hum. Genet. 81, 559–575.

Quinlan, A.R., Hall, I.M., 2010. BEDTools: a flexible suite of utilities for comparing genomic features. Bioinformatics (Oxford, England) 26, 841–842.

Ramskold, D., Wang, E.T., Burge, C.B., Sandberg, R., 2009. An abundance of ubiquitously expressed genes revealed by tissue transcriptome sequence data. PLoS computational biology 5, e1000598.

Raney, B.J., Cline, M.S., Rosenbloom, K.R., Dreszer, T.R., Learned, K., Barber, G.P., Meyer, L.R., Sloan, C.A., Malladi, V.S., Roskin, K.M., Suh, B.B., Hinrichs, A.S., Clawson, H., Zweig, A.S., Kirkup, V., Fujita, P.A., Rhead, B., Smith, K.E., Pohl, A., Kuhn, R.M., Karolchik, D., Haussler, D., Kent, W.J., 2011. ENCODE whole-genome data in the UCSC genome browser (2011 update). Nucleic Acids Res. 39. D871–D871.

Rhodes, J., Lutka, F.A., Jordan-Sciutto, K.L., Bowser, R., 2003. Altered expression and distribution of FAC1 during NGF-induced neurite outgrowth of PC12 cells. Neuroreport 14, 449–452.

Robinson, M.D., McCarthy, D.J., Smyth, G.K., 2010. edgeR: a Bioconductor package for differential expression analysis of digital gene expression data. Bioinformatics (Oxford, England) 26, 139–140.

Roth, R., Hevezi, P., Lee, J., Willhite, D., Lechner, S., Foster, A., Zlotnik, A., 2006. Gene expression analyses reveal molecular relationships among 20 regions of the human CNS. Neurogenetics 7, 67–80.

Sandelin, A., Carninci, P., Lenhard, B., Ponjavic, J., Hayashizaki, Y., Hume, D.A., 2007. Mammalian RNA polymerase II core promoters: insights from genome-wide studies. Nature reviews 8, 424–436.

Schonrock, N., Matamales, M., Ittner, L.M., Jürgen, G., 2011. MicroRNA networks surrounding APP and amyloid-β metabolism–Implications for Alzheimer's disease. Experimental Neurology 235, 447–454.

Shen, J., Bronson, R.T., Chen, D.F., Xia, W., Selkoe, D.J., Tonegawa, S., 1997. Skeletal and CNS defects in presenilin-1-deficient Mice. Cell 89, 629–639.

Starkey, H., Van Kirk, C., Bixler, G., Imperio, C., Kale, V., Serfass, J., Farley, J., Yan, H., Warrington, J., Han, S., Mitschelen, M., Sonntag, W., Freeman, W., 2012. Neuroglial expression of the MHCI pathway and PirB receptor is upregulated in the hippocampus with advanced aging. Journal of Molecular Neuroscience 48, 111–126.

Takahashi, H., Lassmann, T., Murata, M., Carninci, P., 2012. 5' end-centered expression profiling using cap-analysis gene expression and next-generation sequencing. Nat. Protocols 7, 542–561.

Thomas, G.M., Huganir, R.L., 2004. MAPK cascade signalling and synaptic plasticity. Nat. Rev. Neurosci. 5, 173–183.

Thomas, P.D., Campbell, M.J., Kejariwal, A., Mi, H., Karlak, B., Daverman, R., Diemer, K., Muruganujan, A., Narechania, A., 2003. PANTHER: a library of protein families and subfamilies indexed by function. Genome Res. 3, 2129–2141.

Tollervey, J.R., Curk, T., Rogelj, B., Briese, M., Cereda, M., Kayikci, M., Konig, J., Hortobagyi, T., Nishimura, A.L., Zupunski, V., Patani, R., Chandran, S., Rot, G., Zupan, B., Shaw, C.E., Ule, J., 2011. Characterizing the RNA targets and position-dependent splicing regulation by TDP-43. Nat. Neurosci. 14, 452–458.

Tschan, M.P., Fischer, K.M., Fung, V.S., Pirnia, F., Borner, M.M., Fey, M.F., Tobler, A., Torbett, B.E., 2003. Alternative splicing of the human cyclin D-binding Myb-like protein (hDMP1) yields a truncated protein isoform that alters macrophage differentiation patterns. J. Biol. Chem. 19, 42750–42760.

Valen, E., Pascarella, G., Chalk, A., Maeda, N., Kojima, M., Kawazu, C., Murata, M., Nishiyori, H., Lazarevic, D., Motti, D., Marstrand, T.T., Tang, M.H., Zhao, X., Krogh, A., Winther, O., Arakawa, T., Kawai, J., Wells, C., Daub, C., Harbers, M., Hayashizaki, Y., Gustincich, S., Sandelin, A., Carninci, P., 2009. Genome-wide detection and analysis of hippocampus core promoters using DeepCAGE. Genome research 19, 255–265.

Vaquerizas, J.M., Kummerfeld, S.K., Teichmann, S.A., Luscombe, N.M., 2009. A census of human transcription factors: function, expression and evolution. Nature reviews 10, 252–263.

Yerbury, J.J., Poon, S., Meehan, S., Thompson, B., Kumita, J.R., Dobson, C.M., Wilson, M.R., 2007. The extracellular chaperone clusterin influences amyloid formation and toxicity by interacting with prefibrillar structures. Faseb J. 21, 2312–2322.